Electronic structure of GaF_3 films grown on GaAs via exposure to XeF_2

P. R. Varekamp, W. C. Simpson, D. K. Shuh,* T. D. Durbin,† V. Chakarian,‡ and J. A. Yarmoff
Department of Physics, University of California, Riverside, California 92521
and Materials Sciences Division, Lawrence Berkeley Laboratory, Berkeley, California 94720
(Received 2 August 1993; revised manuscript received 31 May 1994)

GaAs(110) and (100) wafers are reacted with XeF_2 at room temperature and studied with soft-x-ray photoelectron spectroscopy (SXPS), photon-stimulated desorption (PSD) and electron-energy-loss spectroscopy (EELS). The reaction between GaAs and XeF_2 results in the homogeneous growth of a GaF_3 film and an interface region consisting of intermediate products. The band gap of GaF_3 and its band lineup with the GaAs substrate are determined via EELS and SXPS. F^+ PSD spectra collected after the initial XeF_2 exposures indicate a single desorption onset at ~28 eV, due to the excitation of a F 2*s* electron to the GaAs conduction-band minimum. PSD spectra collected after larger exposures contain a number of features due to transitions within the GaF_3 band structure. These features appear when the film thickness exceeds ~10 Å, indicating that the bulk electronic structure has developed. Annealing the film to ~250 °C results in the inhomogeneous removal of GaF_3.

I. INTRODUCTION

Many attempts have been made to find a suitable insulator that can be grown on GaAs, but these have not yet led to a process useful to the microelectronics industry.[1] In order for an insulating material to be suitable for device fabrication, it must grow in a spatially homogeneous manner with an interface that is relatively free of gap states. Recently, it has been shown that GaF_3 grown on GaAs satisfies these criteria, and that it can be grown either by GaF_3 deposition or by fluorination of GaAs. To be technologically useful, however, a film growth method should be a simple chemical process, thus eliminating GaF_3 evaporation and placing emphasis on developing a technique for growing GaF_3 via the exposure of GaAs to a F-containing compound. The ease with which a GaF_3 film can be grown via fluorination has been shown previously in reactions of GaAs with F_2,[2,3] F^+ ions,[4] atomic F,[5] CF_4 plasma,[6–9] CHF_3 plasma,[4] and CCl_2F_2 plasma.[10,11] In fact, operational devices have been constructed from GaF_3/GaAs structures, demonstrating that the interface state density can be reduced to a sufficiently low level.[2,3,12–14]

Although electronic devices have been constructed from GaF_3/GaAs, few studies of the fundamental interaction between fluorine and GaAs have been performed and little is known about the electronic structure of the resulting GaF_3 films. In the present work, the reaction of fluorine with GaAs(110) and (100) wafers is studied, concentrating on the electronic structure of the films. XeF_2 is used as the source of atomic fluorine, due to its ease of handling. Film composition is determined by collecting soft-x-ray photoelectron spectroscopy (SXPS) spectra at different stages of the film growth. The films are also examined with electron-energy-loss spectroscopy (EELS) and photon-stimulated desorption (PSD), since these techniques give insight into the electronic structure of the near-surface region.

II. EXPERIMENTAL PROCEDURE

GaAs(110) and (100) samples were etched in a 1:1:200 solution of HNO_3:H_2O_2:H_2O, rinsed with deionized water and then dried with isopropanol before being placed in the ultrahigh vacuum (UHV) chamber. The samples were cleaned in vacuum by sputtering with 500-eV Ar^+ ions, followed by annealing to ~500 °C by resistively heating the Ta foil that held the sample. The sample temperature was determined at a later time by calibrating the annealing current with a chromel-alumel thermocouple, which resulted in an estimated uncertainty of roughly ±50 °C.

Samples were exposed to XeF_2 in a separate UHV dosing chamber which had a base pressure of $\sim 5\times 10^{-10}$ torr. Sample transfers between the dosing chamber and the analysis chamber were performed entirely under UHV. A cold cathode ion gauge was used to monitor the pressure in the dosing chamber in order to prevent the creation of metal fluorides and radical species from the hot filament of a conventional ion gauge. The dosing chamber was passivated with a large amount of XeF_2 prior to any exposures to reduce the likelihood of vapor phase transport of metal fluorides to the sample surface.[15] No evidence of metal contamination was apparent in any of the SXPS spectra collected.

One GaAs(100) and two GaAs(110) samples were used in the SXPS and PSD experiments. All three samples were cleaned and fluorinated in an identical manner. Since no significant differences were observed in the data collected from either crystal face upon exposure to XeF_2, the data from all three samples have been merged. The uptake of XeF_2 was found to vary slightly from sample to sample, however, so that exposures are not readily comparable. For this reason, the gallium fluoride film thickness, instead of the XeF_2 exposure, is reported.

The SXPS and PSD measurements were performed at the National Synchrotron Light Source, Brookhaven Na-

0163-1829/94/50(19)/14267(10)/$06.00 ©1994 The American Physical Society

tional Laboratory, on beamline UV-8a, using an angle-integrating ellipsoidal mirror spectrometer.[16] This analyzer accepts particles within an $\sim 85°$ cone centered about the surface normal. For the collection of the PSD spectra, an additional bias voltage was applied between the sample and the analyzer, which increases the angular acceptance.[17] The photon energy was selected with a 3-m focal length grazing incidence toroidal grating monochromator. The high-resolution SXPS spectra have a combined energy resolution of better than 0.2 eV, and the photon energy resolution in the PSD spectra is <0.3 eV.

In order to ensure that only F^+ ions contribute to the PSD ion yield, electron-stimulated desorption (ESD) experiments were conducted in a separate UHV chamber which was equipped with an electron gun, a hemispherical electrostatic energy analyzer, and a quadrupole mass spectrometer. An electron beam energy of 300 eV was chosen so as to be greater than the highest photon energy used in the collection of the PSD data, which ensures that all of the desorption channels that contributed to the PSD spectra were excited by the electron beam. The same ions are expected to desorb in ESD and PSD, since they are produced by the same mechanisms.[18] With the ionizer of the mass spectrometer off, mass spectra of ESD ions were collected from GaAs(110) wafers prepared and exposed to XeF_2 in the same manner as those used in the collection of the PSD spectra. Only F^+ ions were detected, although the mass spectrometer was not sensitive to H^+. Further experiments ruled out a significant contribution from H^+, however. ESD experiments performed on GaAs exposed to water vapor showed that the kinetic-energy distribution of H^+ is remarkably different from that observed from F/GaAs, and that the total positive ion yield from H_2O/GaAs is over 2 orders of magnitude lower. Hence, any H^+ contribution to the ESD signal from GaAs exposed to XeF_2 is discernible from F^+ and, even if comparable amounts of H and F were present on the surface, the total H^+ signal would constitute less than 1% of the total positive-ion yield.

EELS measurements were carried out in the same UHV chamber used for ESD. The resolution of the EELS measurements was limited to 1.4 eV by the energy width of the 150-eV incident electron beam. All of the EELS spectra presented in this paper were collected from a single GaAs(110) wafer which was prepared and exposed to XeF_2 in the same manner as previously described. Because there is no means of determining the GaF_x film thickness in the EELS apparatus, the spectra are labeled by XeF_2 exposure.

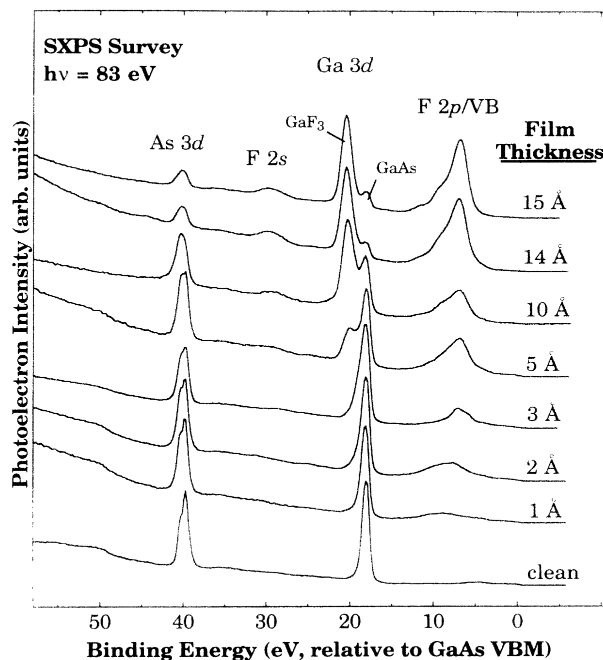

FIG. 1. SXPS survey spectra, containing the valence band and low-lying core levels, for various GaF_x film thicknesses.

III. RESULTS AND DISCUSSION

A. SXPS

SXPS survey spectra, which display the valence band and low-lying core levels, are shown in Fig. 1 in order of increasing film thickness. The binding energies are given with respect to the GaAs valence-band maximum (VBM) which removes any effects due to band bending. This was accomplished by assigning a constant value of 18.6 eV to the Ga $3d_{5/2}$ binding energy (BE) for Ga in bulk GaAs.[19] With increasing XeF_2 exposure, F accumulates on the surface, as indicted by an increase in the intensities of the F $2p$ contribution to the valence band and the appearance of the F $2s$ core level. Following a small exposure to XeF_2, the Ga $3d$ core level broadens toward higher BE. After larger exposures, a distinct second peak appears, which eventually dominates the Ga $3d$ core-level intensity. This second component is attributed to GaF_3.[20] The As $3d$ core level broadens slightly with XeF_2 exposure, and it is attenuated for the largest film thicknesses. These observations are consistent with the formation of a GaF_3 film that covers the underlying substrate and the removal of As from the near-surface region.

Valence-band SXPS spectra collected from GaAs(110) after successive fluorinations are shown in Fig. 2. To display the data on the same intensity scale, each spectrum was divided by the total integrated area of its respective Ga $3d$ core level. This calibration method is appropriate, since the Ga densities in GaAs and GaF_3 are the same to within 5%. The inset of Fig. 2 contains an enlargement of the region near the GaAs VBM for the clean and fluorinated samples and shows that the substrate valence band is continually attenuated with increasing film thickness. There are occupied states in the band gap of the clean surface, due to defects caused by the ion-bombardment cleaning procedure, which are indicted in the inset. These states are quenched after light fluorinations and no new states are observed in the band gap after further fluorination. By extrapolating the high-energy side of the F $2p$ feature down to zero intensity, as indicated with the dashed lines in Fig. 2, it is found that the VBM of the GaF_3 film is located ~ 5.4 eV below

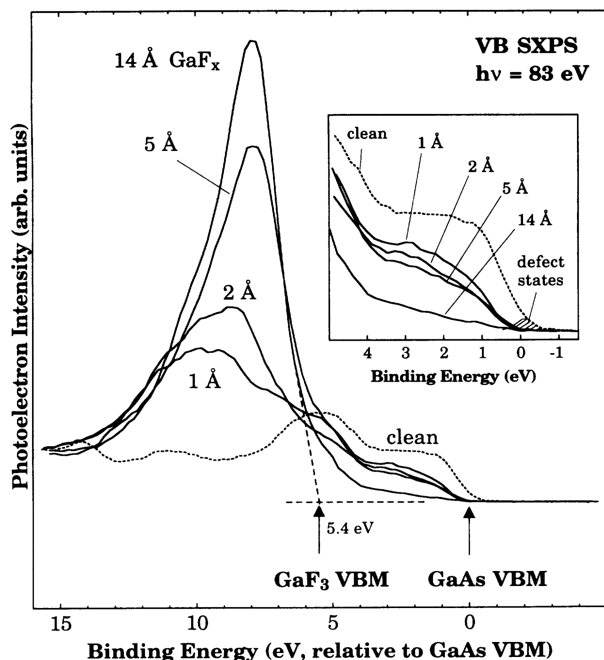

FIG. 2. Valence-band SXPS spectra for various GaF_x film thicknesses, given with respect to the GaAs VBM. The dashed line shows the spectrum collected from the clean GaAs(110) surface, and the solid lines show the spectra collected after successive fluorinations. The inset contains an expanded view of the valence-band edges of the clean and fluorinated samples, which shows the attenuation of the GaAs valence band with increasing film thickness. Extrapolation of the F $2p$ leading edge shows that the GaF_3 VBM is located ~ 5.4 eV below the GaAs VBM.

the GaAs VBM. Note that this rough estimate of the valence-band offset between the film and substrate is confirmed by the EELS measurements reported below. Since the GaF_3 VBM is below the GaAs VBM, and since no significant density of gap states is created by fluorination, the progressive attenuation of the GaAs valence band with increasing film thickness indicates that the film grows in a spatially homogeneous manner. Inhomogeneous film growth, e.g., via island formation, would be indicted by a persistence of the GaAs VBM, which is not observed. The position of the GaF_3 VBM corresponds to the high-energy side of the F $2p$ feature, which dominates the valence band. F $2p$ is expected to mark the VBM for GaF_3, since the uppermost filled states of this nearly ionic solid have primarily F character. A similar correlation between the VBM of the overlayer and F $2p$ was observed for the ionic solid CaF_2 grown on Si(111).[21]

High-resolution Ga $3d$ and As $3d$ core-level spectra, plotted with respect to the substrate $3d_{5/2}$ component, are shown in Figs. 3 and 4 together with numerical fits to the data. The spectra in these two figures were collected from GaAs(110) surfaces. The clean surface spectra are shown in Figs. 3(a) and 4(a), while three representative spectra from fluorinated surfaces are shown in panels (b)–(d). The photon energies were selected so that all the measured photoelectrons have kinetic energies of ~ 35 eV, which maximized the surface sensitivity of the measurement.[22] Using the same photoelectron kinetic energy ensures that both the Ga and As $3d$ spectra indicate the composition of the same part of the near-surface region.

Fluorine uptake varied from sample to sample, and thus the XeF_2 exposure does not accurately reflect the amount of F incorporated into the surface. To better quantify the amount of F present, the GaF_x film thickness was calculated using relative core-level component intensities determined by fitting the high-resolution Ga $3d$ spectra. The calculation is based on the assumption that the bulk Ga signal is attenuated exponentially by a compositionally homogeneous and uniformly thick layer of fluorinated gallium, which is somewhat inaccurate since the film is composed of more than one GaF_x species. It is also assumed that the atomic photoionization cross section of Ga is unchanged by fluorination, and that the photoelectron escape depth is the same for GaAs and GaF_3. It is not the purpose of this calculation to determine an accurate film thickness, however, but rather to allow spectra from several samples, each exposed to a different amount of XeF_2, to be compared. Note that a

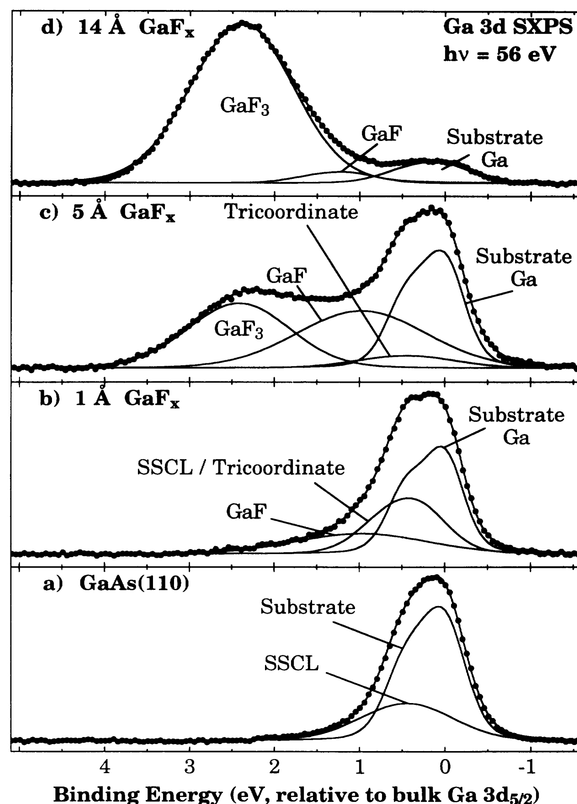

FIG. 3. High-resolution SXPS spectra of the Ga $3d$ core level, collected from GaAs(110) before and after exposure to XeF_2, are shown along with the results of numerical fits to the data. The raw data after background subtraction are shown as solid circles. The solid lines show the individual and the sum of the components of the fit. (a) shows the core level from the clean surface, and (b)–(d) contain core levels from fluorinated surfaces.

correction for differences in the density of Ga atoms in the overlayer and substrate is also not included, but this is acceptable since the densities of Ga in bulk GaF_3 and in bulk GaAs are nearly identical. The film thickness was found from $d = -\Lambda \ln(1-R)$, where R is the ratio of fluorinated Ga to the total Ga 3*d* signal, as determined from the fitting procedure, and Λ is the escape depth of the photoelectrons, which is taken from the literature to be 5.5 Å.[19,22] The film thickness for each spectrum is given in Å of GaF_x ($x = 1-3$) and represents the amount of fluorinated Ga present on the sample.

The Ga 3*d* and As 3*d* core levels were numerically fit, after background subtraction, to a sum of Gaussian-broadened Lorentzian spin-orbit split doublets, using a least-squares optimization routine. A smooth background was determined by fitting a third-order polynomial to each side of the peak. The fitting procedure was used to determine the BE, area, and Gaussian contribution to the width of each core-level component. The Lorentzian full width at half maximum (FWHM) was fixed at 0.12 eV in all of the fits.[23] For the Ga 3*d* core level, the spin-orbit splitting, branching ratio, and the surface core-level shift relative to the bulk component were fixed [for GaAs(110)] at 0.45, 0.66, and 0.28 eV, respectively. For the As 3*d* core level, these parameters were fixed at 0.68, 0.65, and -0.37 eV, respectively. All fitting parameters are consistent with previous treatments of the GaAs(110) surface.[16,20,22,23]

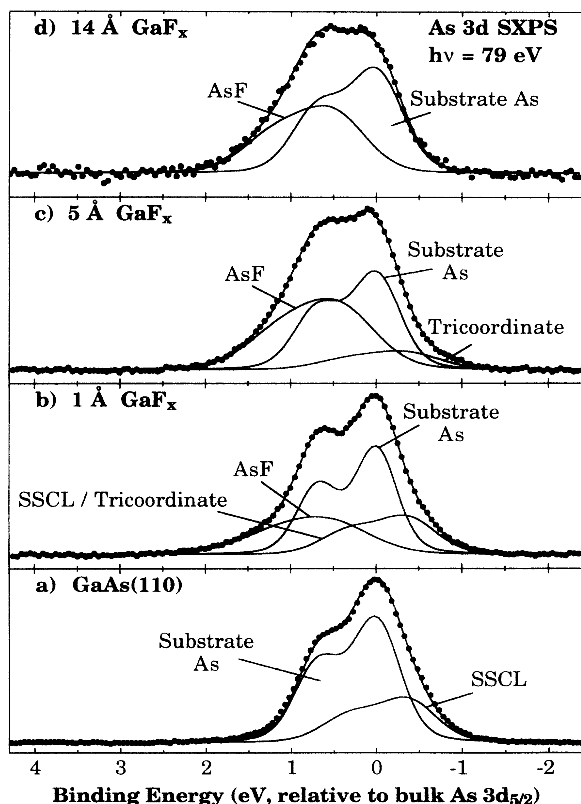

FIG. 4. High-resolution SXPS spectra of the As 3*d* core level, collected from GaAs(110) before and after exposure to XeF_2, are shown along with the results of numerical fits to the data. The raw data after background subtraction are shown as solid circles. The solid lines show the individual and the sum of the components of the fit. (a) shows the core level from the clean surface, and (b)–(d) contain core levels from fluorinated surfaces.

The identification of the chemically shifted components in the Ga 3*d* core-level spectra as GaF and GaF_3, has been made previously.[4,6,12,20] Note that good fits were achieved for all of the Ga 3*d* core-level spectra by only including two reacted components. It was not necessary to include any additional components, such as one for GaF_2, although the presence of some GaF_2 on the surface cannot be ruled out. In the fits to core-level spectra collected after small XeF_2 exposures, the GaF BE was fixed at 0.8 eV relative to the substrate.[20] However, the relative BE's for both GaF and GaF_3 increase slightly with exposure, presumably due to the decrease in screening as the insulating GaF_3 overlayer thickens.[24,25]

As shown in Fig. 4, there are relatively few changes in the As 3*d* core level as a function of XeF_2 exposure. The intensity of the high BE side gradually increases with fluorination, which indicates that there is at least one As reaction product present. The inclusion of only one reacted component was sufficient to achieve good fits in all of the As 3*d* spectra collected. This high BE component is consistent with either AsF or elemental As.[20,22,26–28] Note that the lower signal-to-noise ratio in Fig. 4(d) is a consequence of the reduction of the total As 3*d* signal due to the removal of As from the near-surface region.

In the fitting procedure employed here, the Gaussian widths of the surface-shifted core-level (SSCL) components were treated as independent parameters. In many fits to high-resolution core levels for GaAs surfaces, however, the Gaussian widths of the substrate and surface components have been constrained to be equal.[19,23,26] For a cleaved surface, this assumption may be justified, but in this study of sputtered and annealed wafers the constraint was relaxed. As shown in Figs. 3(a) and 4(a), relaxing this constraint results in a surface component that is significantly broader than the substrate component. This broadening is likely due to presence of additional defects and variations in the electronic environments of surface atoms on an ion-bombarded and annealed wafer, resulting in a larger Gaussian width for the surface component.[20,29]

To achieve good fits to the 3*d* spectra collected from films as thick as 5 Å, it was necessary to include components shifted in BE ~ 0.3 eV and ~ -0.4 eV from the Ga and As substrate peaks, respectively. For clean GaAs(110), these are due to surface atoms, and are labeled as SSCL's. A similar persistence of the SSCL with exposure was also seen for cleaved GaAs(110) exposed to XeF_2 and to Cl_2.[20,30] Considering the high reactivity of fluorine and chlorine, it is unlikely that there are enough unreacted regions of the GaAs surface left after large exposures to account for the intensity of these components. More likely, the SSCL's in spectra collected from reacted samples have an additional contribution from other species that have similar BE shifts.

Surface Ga and As atoms on GaAs(110) are in a tri-

coordinate geometry, with one less bond than substrate atoms, resulting in their observed BE shifts. It is reasonable to assume that any tricoordinate Ga and As atoms created in the substrate during the reaction would exhibit BE shifts similar to those of the surface atoms, and thus the two would be indistinguishable. If this is the case, then the persistence of the SSCL can be explained by tricoordinate Ga and As atoms generated in the substrate as a result of bond breaking during halogenation. For the F/GaAs reaction, it is expected that these buried tricoordinate atoms are located at the film-substrate interface, where the reaction occurs, and that they are continually created and removed as the film grows.

The behavior of the Ga 3*d* and As 3*d* core levels of GaAs(110) cleaves exposed to XeF_2 is virtually identical to that observed for GaAs(110) and (100) wafers, even though the composition of the initial clean surfaces is quite different.[20] Cleaved GaAs(110) has a well-known structure,[31,32] with equal amounts of Ga and As at the surface. Sputtered (110) wafers are slightly Ga rich due to the higher sputtering rate of As,[33,34] although annealing may nearly restore the 1:1 Ga:As ratio to the surface since As diffuses easily at elevated temperatures.[35] Several different Ga-terminated surfaces can result from annealing a GaAs(100) wafer in vacuum following sputtering. Each reconstruction has a different As content, but all are Ga rich.[36] Even though annealing may restore much of their surface crystallinity, the samples used in this study still have a number of defects on the surface, indicated by the presence of the defect states shown in the inset of Fig. 2. Since the behavior of the core levels upon fluorination was the same for the cleaves and the wafers, but the starting surfaces were quite different, the initial surface order and crystal face does not appear to be important in determining the surface products generated in the F/GaAs reaction. This is likely due to the fact that the GaF_3 films grow by etching down into the GaAs substrate, so that the composition of the film is relatively insensitive to the amount of crystallinity originally present and to the crystal orientation.

B. EELS

In order to probe unoccupied electronic states, EELS measurements were carried out on a clean GaAs(110) wafer and on the same wafer after exposure to increasing amounts of XeF_2. The results of these measurements are shown in Fig. 5, in which each spectrum has been normalized to its elastic peak intensity. The two strong loss features visible in the EELS spectra at 6.8 and 9.8 eV are due to the excitation of electrons from the valence band of GaF_3. Their intensity is relatively high since the GaF_3 valence band has a large density of states due to F 2*p* (see Fig. 1). The 6.8-eV loss feature is assigned to the transition from the GaF_3 VBM to the GaAs conduction-band minimum (CBM). Since the GaAs band gap is 1.4 eV, this indicates that the valence-band offset between GaAs and GaF_3 is 5.4 eV, confirming the value determined from SXPS (Fig. 2). The 9.8-eV loss is due to the transition across the GaF_3 band gap and is consistent with an earlier optical absorption measurement of 9.6 eV.[12] The

FIG. 5. EELS spectra collected from a GaAs(110) wafer, and from the same wafer after increasing exposures to XeF_2. The combined resolution of the electron beam and detector is 1.4 eV. Two loss features at 6.8 and 9.8 eV are apparent in the spectra collected from the fluorinated samples, and correspond to transitions from the GaF_3 VBM to the GaAs CBM and GaF_3 CBM, respectively.

FIG. 6. The band lineup, based on the SXPS and EELS measurements, of GaF_3 films grown on GaAs wafers via exposure to XeF_2. The energies of the band edges are given with respect to the GaAs VBM. The electronic transitions responsible for the EELS features are indicated.

overlayer-substrate band lineup, and the two electronic transitions observed in EELS are illustrated in Fig. 6.

Further support for the assignment of the two loss features is obtained from their behavior as a function of XeF_2 exposure. It is seen in Fig. 5 that the 6.8-eV feature diminishes in intensity for the highest fluorination levels, and thus for the thickest films, which is expected for a feature that results from a transition localized at the film-substrate interface. The intensity of the 6.8-eV feature is not completely attenuated, however, since the escape depth of ~150-eV electrons is on the order of the thickness of the films. Thus, all of the EELS spectra reported here have contributions from both the film and the interface. The increase in the intensity of the 9.8-eV loss feature with increasing fluorination is consistent with excitation across the GaF_3 band gap, since the transition occurs solely within the GaF_3 film.

C. PSD

Figure 7 shows PSD spectra collected from GaAs as a function of exposure to XeF_2. Each spectrum was collected by ramping the photon energy and detecting the total yield of positive ions. Unless otherwise stated, all of the features in the spectra result from first-order light from the monochromator. The PSD spectra are divided into two exposure regimes which exhibit qualitatively different behavior. In the low exposure regime, which includes GaF_x films up to 5 Å thick, there is primarily one feature with a peak located at ~34 eV and an onset at ~28 eV. At a film thickness of 5 Å, a shoulder develops at ~30 eV, signaling the onset of PSD features characteristic of the high-exposure regime. There are a large number of features in the high-exposure regime that remain mostly unchanged with increasing film thickness. The similarity of the spectra in the high-exposure regime gives an indication of the reproducibility of PSD collected from heavily fluorinated GaAs, since each spectrum was collected from a different sample.

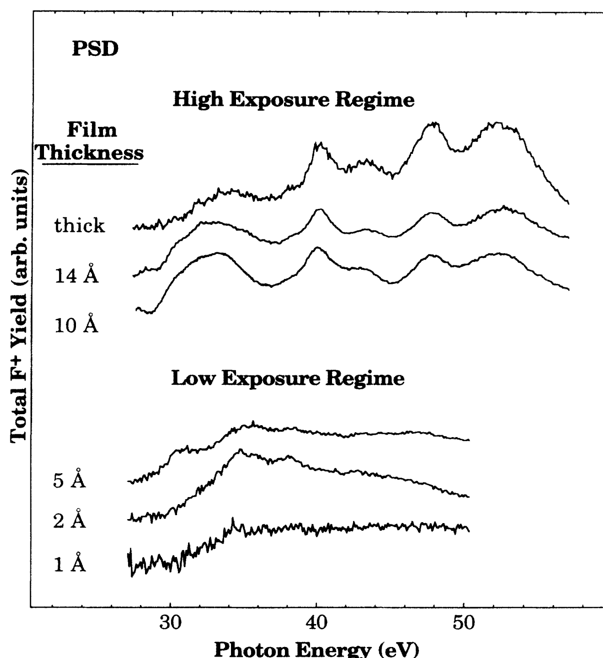

FIG. 7. Total F^+ PSD yield shown as a function of photon energy for various film thicknesses. The spectra are divided into two exposure regimes. All of the spectra in the low-exposure regime were collected from the same GaAs(110) sample. In order of increasing film thickness, the spectra in the high-exposure regime were collected from a (100) sample, the same (110) sample as the low-exposure regime spectra, and a different (110) sample.

To determine if some of the PSD features in the high-exposure regime are due to electronic transitions within the film-substrate interface, a thick film was grown by exposing a GaAs(110) wafer to the vapor pressure of XeF_2 (~4 torr) for 10^3 sec. Due to problems with sample charging during measurement, the thickness of the film could not be determined. However, there is no detectable contribution from As 3*d* in the survey spectrum, which indicates that the GaF_3 film is at least ~40 Å thick. For the photon energies used, a 40-Å-thick film would result in 99.9% attenuation of the As 3*d* signal originating from the bulk and interface, thus making the As 3*d* signal comparable to the noise level. Note that the reduced signal to noise in the PSD spectrum collected from the thick film is due to sample charging.

The features in the PSD spectra of Fig. 7 are due to photon-induced electronic transitions that lead to ion desorption. The mechanism responsible for PSD of F^+ ions in this system begins with the formation of a core hole via photoabsorption. The filling of this core hole via an Auger process produces a long-lived repulsive state that ultimately leads to the desorption of a F^+ ion.[37] The total F^+ yield is collected as a function of photon energy in order to determine the correlation between the formation of certain core holes and the creation of ions. Because F is more electronegative than Ga or As, the formation of a F-Ga or F-As bond results in charge transfer that leaves F with a partial negative charge. Thus, only those processes that remove at least two electrons from a F atom will lead to F^+ desorption. Because of this constraint, Ga and As core holes must be filled via interatomic Auger decay in order to create a F^+ ion, whereas a F core hole must be filled via intra-atomic Auger decay. Note that the cross sections for these two decay processes can be widely different, depending on the ionicity of the bond. Also, in order to have a detectable ion yield, the resulting repulsive states must have a sufficiently long lifetime, and the Auger decay process that leads to a repulsive state cannot be overwhelmed by competing processes.

The initial excitation responsible for the onset of PSD in the low exposure regime was identified by comparing a PSD spectrum to an SXPS survey spectrum, as shown in Fig. 8. The SXPS spectrum is plotted relative to the GaAs CBM, since this is the lowest unoccupied state and is thus the most likely final state for an electronic transition. The dashed vertical line shows that the onset of PSD occurs at the same energy as the BE of the F 2*s* initial state. This correlation between the F 2*s* level in the SXPS spectrum and the feature in the PSD spectrum indicates that the electronic transition responsible for the

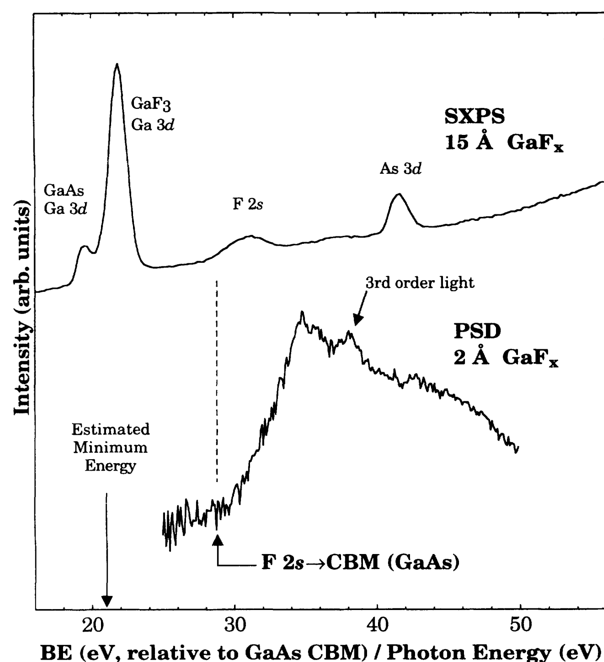

FIG. 8. Comparison of a low-exposure regime PSD spectrum collected from a 2-Å film to a SXPS survey spectrum collected from a 15-Å film. The SXPS spectrum is given with respect to the GaAs CBM to facilitate the identification of the PSD feature. The vertical dashed line shows the onset of the PSD feature. Note that a SXPS survey spectrum from the high-exposure regime was used for comparison so that the F 2*s* core level is more prominent. The PSD feature at 38 eV is due to third-order light from the monochromator ionizing the Ga 3*p* core level.

onset of F^+ PSD in the low exposure regime is the promotion of a F 2*s* electron to the GaAs CBM. Note that the small feature located at $\sim$38 eV is due to ionization of the Ga 3*p* core level by third-order light from the monochromator. Also note that, because of the low intensity of F 2*s* in the low-exposure regime, a SXPS survey spectrum from the high-exposure regime was used for the comparison in this figure, which is valid because the F 2*s* BE does not change significantly with fluorination.

In order for a single photon to induce the desorption of F^+, it must at least have the minimum energy required to break the F-substrate bond, ionize the F atom, and remove it from the surface.[38] The calculated energy threshold for a single photon to induce desorption in this system is $\sim$21 eV, and is indicted in Fig. 8. The actual threshold, however, is located at the F 2*s* absorption edge, which also marks the threshold for the desorption of F^+ from Si.[39–41] One reason that there is little structure in the low-exposure regime PSD spectra is that the energy required to ionize the Ga 3*d* core level in GaAs ($\sim$20 eV) is not sufficiently above the energy threshold necessary to induce ion desorption. Thus, transitions from Ga 3*d* initial states do not make a significant contribution to the PSD signal.

In addition, electronic transitions with an As 3*d* initial state do not appear to induce PSD. The identity of the As product generated in the F/GaAs reaction cannot be determined conclusively, since its chemical shift is consistent with that of either elemental As or AsF. If only elemental As is produced in the reaction, then As 3*d* initial states would not induce PSD since there would be no F bonded to As. However, if AsF is produced by the reaction, PSD induced by transitions from As 3*d* initial states may be suppressed because the As-F bond is more covalent than Ga-F. With less charge transferred to the F atom, the cross section for filling the As core hole via an intra-atomic Auger process can compete with the interatomic Auger decay, thereby reducing the probability for creating F^+. Moreover, even if a F^+ ion were produced via the formation of an As 3*d* core hole, the resulting repulsive state may not have a long enough lifetime to result in PSD.

Since PSD spectra reflect the electronic transitions that occur in the near-surface region, the change in the spectra between the low- and high-exposure regimes indicates that a change in the electronic structure has occurred. As determined from SXPS, GaF_3 first appears in the 5-Å-thick film, and GaF_3 becomes the dominant surface species once the film thickness reaches 10 Å. Likewise, a close examination of the PSD spectra in Fig. 7 shows that the features in the high-exposure regime are just starting to form in the spectrum collected from the 5-Å-thick film, and that they are fully formed by the 10 Å. Thus, the most reasonable explanation for the change in the PSD spectra is that there is sufficient GaF_3 present on the surface for it to possess the electronic structure of bulk GaF_3. The PSD features in the high-exposure regime are then expected to be due to electronic transitions within the GaF_3 band structure. It should be noted that the feature in the low-exposure regime, which is caused by the promotion of a F 2*s* electron to the GaAs CBM, is not observed in the high-exposure regime, because the F bonded to the substrate is covered by $\sim$10 Å or more of GaF_x. Any F^+ ions generated by excitation to the GaAs CBM would have to travel through the GaF_x overlayer, and are likely to be neutralized before escaping the surface.

Although the PSD features in the high-exposure regime cannot be identified as simply as in the low-exposure regime, there is sufficient information that can be used to assign transitions to each feature. These features, labeled *A*–*F*, are shown in Fig. 9, in which a PSD spectrum is compared to a SXPS survey spectrum plotted relative to three possible final states. Since the only atomic species present at the outermost surface are F and Ga, the features in the PSD spectrum must be due to transitions from Ga 3*d* and F 2*s* initial states, and thus, for clarity, only the F 2*s* and Ga 3*d* portion of the SXPS spectrum is shown.

The assumption of the existence of three final states, located 5.9, 15.0, and 18.3 eV above the GaF_3 CBM, leads to a simple and consistent identification of the transitions responsible for PSD features *A*–*F*. First, note that there are no transitions directly to the GaF_3 CBM that induce PSD. However, it can be concluded that PSD feature *A*,

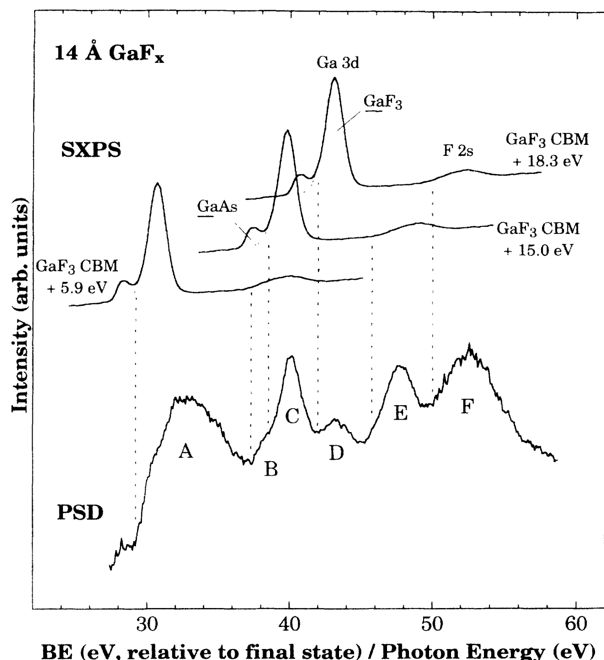

FIG. 9. Comparison of a high-exposure regime PSD spectrum to a SXPS survey spectrum, both collected from a 14-Å-thick film. The SXPS spectrum is given with respect to three unoccupied states in GaF_3 located 5.9, 15.0, and 18.3 eV above the GaF_3 CBM. Transitions from Ga 3*d* and F 2*s* initial states to these three final states lead to the six observed PSD features, *A*–*F*. Dashed lines indicate the threshold of each transition.

located between 30 and 38 eV, is due to the ionization of a Ga 3*d* electron, since this is the only core level with a BE low enough to be the initial state. If the Ga 3*d* in GaF_3 is the initial state for the transition represented by PSD feature *A*, then, in order to explain the location and width of the feature, there must be an ~4-eV-wide band of final states starting about 5.9 eV above the GaF_3 CBM. It is then assumed that a transition from the F 2*s* level to this band also induces PSD, which explains feature *B*, which has an onset at ~38 eV and extends beneath the sharper features *C* and *D*. Second, since PSD feature *C* is narrower than the F 2*s* level, it must be due to a transition from the GaF_3 Ga 3*d* initial state. This implies that there is a sharp final state located 15.0 eV above the GaF_3 CBM. A F 2*s* transition to this state is then responsible for PSD feature *E*, which is centered at ~48 eV. Finally, the spacing and widths of the remaining two features, *D* and *F*, are consistent with transitions from the Ga 3*d* and the F 2*s*, respectively, to a state located 18.3 eV above the GaF_3 CBM. Thus, the existence of three final states in the GaF_3 electronic structure is postulated in order to explain the observed PSD features in a manner that is simple and consistent with the data. Further measurements or theoretical work, e.g., GaF_3 band-structure calculations, are needed to confirm the existence of these states.

It is interesting to note that, for this system, both cation and anion excitations induce F^+ PSD, similar to F/Si,[17,41] and that both types of excitation have comparable ion yields (see Fig. 7). This is in contrast to the CaF_2 system, for example, in which the Ca-F bond is so ionic that only cation excitations lead to measurable F^+ PSD,[42] or the Cl_2/Si system, which is more covalently bonded, resulting in only anion excitations leading to Cl^+ PSD.[43] The fact that the ion yields for both types of excitation are comparable is probably due to the Ga-F bond in GaF_3 being less ionic than the Ca-F bond in CaF_2 but more ionic than the Si-Cl bond.

It was mentioned earlier that the SXPS spectra indicate that the reaction product distribution in the film is independent of the initial surface structure or surface orientation. Likewise, the similarity of the three high-exposure regime PSD spectra of Fig. 7 indicates that the electronic properties of the GaF_3 film are independent of the initial GaAs crystal face, since the spectra in this figure were collected from both GaAs(110) and (100). This is because the observed PSD features in this regime reflect the electronic structure of GaF_3, and have little to do with the underlying substrate.

D. Annealing GaF_3 films

Figure 10 shows Ga 3*d* SXPS spectra collected from (a) GaAs(100) covered with a 9.8-Å-thick film, (b) the same surface after annealing to ~175 °C, and (c) after annealing to ~250 °C. The Ga 3*d* core levels were fit in the same manner as those in Fig. 3, and show that the relative intensity of the GaF_3 component continually decreases with each anneal. Note that, although the intensity of this component is very small after the 250 °C anneal, the presence of a GaF_3 component is required in order to produce an acceptable BE for the GaF component in fitting the spectrum.

Figure 11 shows PSD spectra collected from these same surfaces. Although the PSD features broaden and decrease in intensity with annealing, there are features indicative of the high-exposure regime present even after the highest temperature anneal, which indicates that some bulk GaF_3 band structure still exists. Figure 10(c) shows, however, that the film does not contain enough fluorinated Ga to have the uniform thickness of 10 Å required for a film to possess a GaF_3 band structure.

The presence of GaF_3 band structure in a film that appears to contain very little GaF_3 can be explained by the inhomogeneous rearrangement, or removal, of GaF_3 upon annealing. This immediately explains the broadening and other small changes in the high-exposure regime PSD features, since the PSD signal contains contributions from many regions with different film thicknesses. The rearrangement of GaF_3 on the surface, via diffusion, could create islands of GaF_3 that are thicker than the original film, and which coexist with areas of exposed GaAs substrate. This would explain both the SXPS data, where the substrate Ga component contributes substantially to the Ga 3*d* core level after annealing, and the PSD data, since F^+ ions would still be produced at the surface of the GaF_3 islands. However, a change of the GaF_3 signal from 58% of the total Ga 3*d* intensity to 7%

solely due to a rearrangement of the film is not likely. A more plausible explanation is that some of the film is removed by evaporation, resulting in the formation of holes in an otherwise uniformly thick GaF_3 film, possibly similar to those seen when SiO_2 films grown on Si are annealed.[44] Note that, due to the inhomogeneity of the film's removal, the thicknesses given in parts (c) and (d) of Figs. 10 and 11 only represent the relative amount of fluorinated Ga observed in the SXPS spectra, and are not directly comparable to other film thicknesses given in this paper. Although the highest annealing temperature only begins to approach the $\sim 800\,^{\circ}C$ sublimation temperature of GaF_3,[45] it is believed that the film evaporates as molecular GaF_3, even at the lower temperatures used in this experiment, since there is no evidence in the SXPS data to indicate the decomposition of GaF_3.

IV. SUMMARY

GaAs(110) and (100) surfaces were exposed at room temperature to XeF_2 and studied with SXPS, EELS, and PSD. The reaction between GaAs and XeF_2 results in the homogeneous growth of GaF_3. Between the GaF_3 and GaAs, there is an interface region consisting of GaF, AsF and/or elemental As, as well as tricoordinate Ga and As atoms. Neither the initial surface order nor the crystal face affects the distribution of surface products generated in the reaction. The band gap of the films and the band lineup of the films with the GaAs substrate were determined from EELS and from the SXPS valence-band spectra. F^+ PSD spectra collected after the initial XeF_2 exposures contain a single onset at ~ 28 eV, corresponding to the excitation of a F 2*s* electron to the GaAs CBM. PSD spectra collected after larger exposures contain a number of features, attributed to transitions within the GaF_3 band structure, thus providing a soft-x-ray absorption spectrum of solid GaF_3. These features appear when the film thickness exceeds ~ 10 Å, indicating that the films have developed the electronic band structure of bulk GaF_3. Annealing the films to $\sim 250\,^{\circ}C$ causes the inhomogeneous removal of GaF_3, resulting in surfaces that still possess some GaF_3 band structure in spite of the near absence of GaF_3.

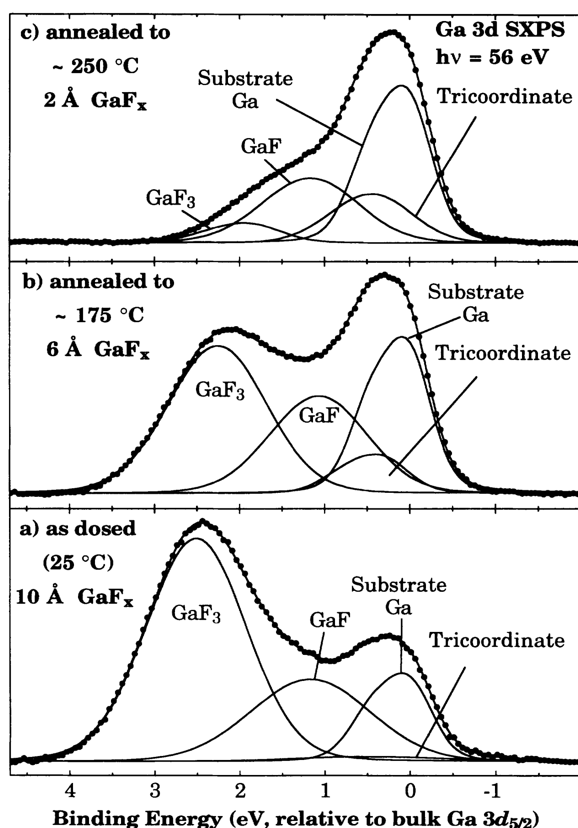

FIG. 10. High-resolution SXPS spectra of the Ga 3*d* core level collected from (a) a GaAs(100) sample dosed with XeF_2 to create a 10-Å-thick film, (b) the sample annealed to $\sim 175\,^{\circ}C$, and (c) the sample further annealed to $\sim 250\,^{\circ}C$. The solid circles in each panel show the raw data after background subtraction. The solid lines show each component of a numerical fit to the data and the sum of all the components.

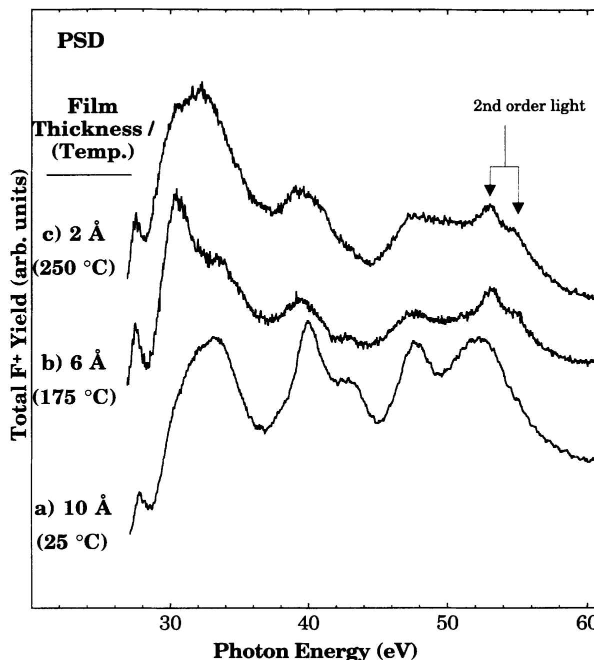

FIG. 11. PSD spectra collected from the same surfaces as in Fig. 10. The PSD features in (b) and (c) marked with arrows are due to ionization of the Ga 3*p* core level by second-order light from the monochromator.

ACKNOWLEDGMENTS

Acknowledgment is made to the Donors of The Petroleum Research Fund, administered by the American Chemical Society, for the partial support of this research. This work was supported by the Director, Office of Energy Research, Office of Basic Energy Sciences, Materials Sciences Division of the U.S. Department of Energy un-

der Contract No. DE-AC03-76SF00098. This work was conducted, in part, at the National Synchrotron Light Source, Brookhaven National Laboratory, which is supported by the Department of Energy (Division of Materials Sciences and Division of Chemical Sciences, Basic Energy Sciences) under Contract No. DE-AC02-76CH00016. The authors also acknowledge F. A. Houle for useful discussions and for providing samples.

---

*Present address: Chemical Sciences Division, Lawrence Berkeley Laboratory, Berkeley, CA 94720.

†Present address: College of Engineering, Center for Environmental Research and Technology, University of California, Riverside, CA 92521.

‡Present address: Naval Research Laboratory, Code 6345, Washington, D.C. 20375.

[1]W. F. Croydon and E. H. C. Parker, *Dielectric Films on Gallium Arsenide* (Gordon and Breach, New York, 1981).

[2]A. S. Barrière, B. Desbat, H. Guégan, L. Lozano, T. Séguelong, A. Tressaud, and P. Alnot, Thin Solid Films **170**, 259 (1989).

[3]A. S. Barrière, G. Couturier, H Guégan, T. Séguelong, A. Thabti, P. Alnot, and J. Chazelas, Appl. Surf. Sci. **41/42**, 383 (1989).

[4]L. R. Williston, I. Bello, and W. M. Lau, J. Vac. Sci. Technol. A **10**, 1365 (1992).

[5]A. Freedman and C. D. Stinespring, J. Phys. Chem. **96**, 2253 (1992).

[6]R. W. Bernstein and J. K. Grepstad, J. Appl. Phys. **68**, 4811 (1990).

[7]M. Taniguchi, T. Murakawa, and Y. Kajitani, Appl. Surf. Sci. **56-58**, 827 (1992).

[8]P. Alnot, J. Olivier, F. Wyczisk, and R. Joubard, J. Electrochem. Soc. **136**, 2361 (1989).

[9]J. Olivier, P. Alnot, and R. Joubard, in *Plasma-Surface Interaction and Processing of Materials,* Vol. 176 of *NATO Advanced Study Institute* (Kluwer Academic, Boston, 1990).

[10]K. L. Seaward, N. J. Moll, D. J. Coulman, and W. F. Stickle, J. Appl. Phys. **61**, 2358 (1987).

[11]M. Meyyappan, G. F. McLane, M. W. Cole, R. Laraeu, M. Namaroff, J. Sasserath, and C. S. Sundararaman, J. Vac. Sci. Technol. A **10**, 1147 (1992).

[12]A. S. Barrière, G. Couturier, G. Gevers, H. Guégan, T. Séguelong, A. Thabti, and D. Bertault, Thin Solid Films **173**, 243 (1989).

[13]H. Ricard, K. H. Kim, K. Aizawa, and H. Ishiwara, Jpn. J. Appl. Phys. **29**, L2460 (1990).

[14]H. Ricard, K. Aizawa, and H. Ishiwara, Appl. Surf. Sci. **56-58**, 888 (1992).

[15]C. W. Lo, D. K. Shuh, V. Chakarian, T. D. Durbin, P. R. Varekamp, and J. A. Yarmoff, Phys. Rev. B **47**, 15 648 (1993).

[16]D. E. Eastman, J. J. Donelon, N. C. Hien, and F. J. Himpsel, Nucl. Instrum. Methods **172**, 327 (1980).

[17]J. A. Yarmoff and S. A. Joyce, Phys. Rev. B **40**, 3143 (1989).

[18]D. P. Woodruff, P. D. Johnson, M. M. Traum, H. H. Farrell, N. V. Smith, R. L. Benbow, and Z. Hurych, Surf. Sci. **104**, 282 (1981).

[19]D. E. Eastman, T.-C. Chiang, P. Heimann, and F. J. Himpsel, Phys. Rev. Lett. **45**, 656 (1980).

[20]A. B. McLean, L. J. Terminello, and F. R. McFeely, Phys. Rev. B **40**, 11 778 (1989).

[21]D. Rieger, F. J. Himpsel, U. O. Karlsson, F. R. McFeely, J. F. Morar, and J. A. Yarmoff, Phys. Rev. B **34**, 7295 (1986).

[22]P. K. Larsen, J. H. Neve, J. F. van der Veen, P. J. Dobson, and B. A. Joyce, Phys. Rev. B **27**, 4966 (1983).

[23]A. B. McLean, Surf. Sci. **220**, L671 (1989).

[24]D. P. Woodruff and T. A. Delchar, *Modern Techniques of Surface Science* (Cambridge University Press, Cambridge, 1986).

[25]G. Hollinger and F. J. Himpsel, Appl. Phys. Lett. **44**, 93 (1984).

[26]A. D. Katnani, H. W. Sang, Jr., P. Chiaradia, and R. S. Bauer, J. Vac. Sci. Technol. B **3**, 608 (1985).

[27]G. P. Schwartz, G. J. Gualtieri, G. W. Kammlott, and B. Schwartz, J. Electrochem. Soc. **126**, 1739 (1979).

[28]J. F. van der Veen, P. K. Larsen, J. H. Neave, and B. A. Joyce, Solid State Commun. **49**, 659 (1984).

[29]G. Landgren, R. Ludeke, Y. Jugnet, J. F. Morar, and F. J. Himpsel, J. Vac. Sci. Technol. B **2**, 351 (1984).

[30]D. K. Shuh, C. W. Lo, J. A. Yarmoff, A. Santoni, L. J. Terminello, and F. R. McFeely, Surf. Sci. **303**, 89 (1994).

[31]R. M. Feenstra, J. A. Stroscio, J. Tersoff, and A. P. Fein, Phys. Rev. Lett. **58**, 1192 (1987).

[32]R. Moller, J. Fraxedas, C. Baur, B. Koslowski, and K. Dransfeld, Surf. Sci. **269/270**, 817 (1992).

[33]I. L. Singer, J. S. Mudray, and L. K. Cooper, Surf. Sci. **108**, 7 (1981).

[34]A. van Oostrom, J. Vac. Sci. Technol. **13**, 224 (1976).

[35]W. Monch, in *Molecular Beam Epitaxy and Heterostructures,* edited by L. L. Chang and K. Ploog (Martinus Nijhoff, Boston, 1987).

[36]M. A. Mendez, F. J. Palomares, M. T. Cuberes, J. L. Gonzalez, and F. Soria, Surf. Sci. **251/252**, 145 (1991).

[37]M. L. Knotek, Rep. Prog. Phys. **47**, 1499 (1984).

[38]T. E. Madey and J. T. Yates, Jr., J. Vac. Sci. Technol. **8**, 525 (1971).

[39]M. J. Bozack, M. J. Dresser, W. J. Choyke, P. A. Taylor, and J. T. Yates, Jr., Surf. Sci. **184**, L332 (1987).

[40]P. Avouris, F. Bozso, and A. R. Rossi, in *Photon Beam and Plasma Stimulated Chemical Processes at Surfaces,* edited by V. M. Donnelly, I. P. Herman, and M. Hirose, MRS Symposia Proceedings No. 75 (Materials Research Society, Pittsburg, 1987).

[41]J. A. Yarmoff, D. K. Shuh, V. Chakarian, T. D. Durbin, K. A. H. German, and C. W. Lo, in *Desorption Induced by Electron Transitions DIET V,* edited by A. R. Burns, E. B. Stechel, and D. R. Jennison (Springer-Verlag, Berlin, 1993), p. 253.

[42]V. Chakarian, T. D. Durbin, P. R. Varekamp, and J. A. Yarmoff, Phys. Rev. B **48**, 18 332 (1993).

[43]T. D. Durbin, W. C. Simpson, V. Chakarian, D. K. Shuh, P. R. Varekamp, C. W. Lo, and J. A. Yarmoff, Surf. Sci. (to be published).

[44]R. Tromp, G. W. Rubloff, P. Balk, F. K. L. Goues, and E. J. van Loenen, Phys. Rev. Lett. **55**, 2332 (1985).

[45]D. R. Lide, *Handbook of Chemistry and Physics* (Commerical Rubber, Boca Raton, 1992).